

Modelling the response of a vibrating-element density meter in a two-phase mixture

By JOHN BILLINGHAM

Department of Mathematics and Statistics, The University of Birmingham, Edgbaston,
Birmingham B15 2TT, UK

(Received 25 January 1996 and in revised form 9 September 1996)

A vibrating-element density meter is a mechanical oscillator with known properties, for example a tuning fork or a simple rod, driven to vibrate at a known frequency. The oscillator is immersed in a fluid and the resonant frequency measured. The density of the fluid can then be inferred. We consider an idealized meter immersed in two-phase flows of various types, and investigate whether a simple single-phase interpretation allows us to deduce the density of the mixture. We find that, when the density contrast between the two fluids is not great, the simple interpretation gives good results, for example in oil/water flows. However, when the density contrast is significant, for example in gas/liquid flows, the simple interpretation is highly inaccurate.

1. Introduction

The use of vibrating-element meters to measure the density of a single fluid is widespread, and has a number of significant advantages over other methods. (a) Very little bulk motion is generated in the fluid. (b) The vibrating part of the device can be small (a few centimetres long). (c) Little heat is generated during the measurement. (d) The principal measurements can be reduced to those of mass, length and time, which can be made with high precision. (e) The measurement can be made in a high pressure environment.

The measurement principle employed is straightforward. A mechanical oscillator, such as a tuning fork or simple rod, is driven to oscillate at a known frequency when surrounded by the fluid whose density is sought, and the resonant frequency determined. The amount by which the resonant frequency is shifted from that determined *in vacuo* is a known function of the density of the fluid, which can then be inferred. A similar measurement can also be used to measure the viscosity of the fluid, although the design parameters of the device may be somewhat different. If the system is set up so that there is a change of phase in the oscillation of the device along its length, for example a standing wave, then it may be possible to deduce the longitudinal flow rate of the fluid by measuring the amount by which the phase of the response is changed by the flow. This type of device is often known as a Coriolis meter.

In this paper we consider the operation of a vibrating-element meter in a flowing mixture of two different fluids. We shall restrict our attention to the possibility of measuring the fluid mixture density, and hence of deducing the fraction of each fluid phase from their known densities. Multiphase flows arise in various contexts, notably in the oil and nuclear industries, but also in many chemical engineering processes. A measurement of the phase fractions in a two-phase mixture is often important, but

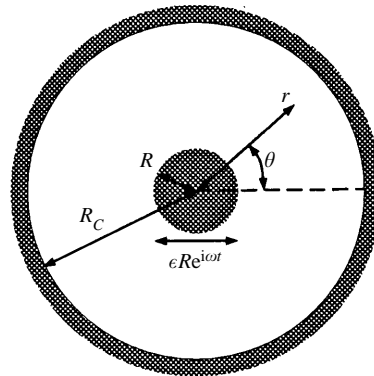


FIGURE 1. The coordinate system for a rod vibrating in a pipe containing a fluid.

never easy. A good example is the oil/water flow that must be metered downhole in a producing oil well, where the temperature and pressure are high. Vibrating-element meters are used on some platforms in the North Sea to meter the mass flow rate and density of flows leaving the gas/liquid separator and consisting mainly of oil and water. There is, however, little experimental or theoretical work available to give the user any confidence in the operation of these devices in such a flow (see, for example, Watt & Lu 1992).

2. A model problem

The aim of this paper is to gain some insight into whether the response of a vibrating-element density meter is likely to be interpretable in a two-phase flow. In order to achieve this, we consider the model problem illustrated in figure 1. An infinitely long solid rod of radius R vibrates uniformly in the direction $\theta = 0$ with angular frequency ω and amplitude ϵR in a rigid pipe with radius R_C . The pipe contains two fluids, labelled fluid 1 and fluid 2, with densities ρ_1 and ρ_2 respectively. We also assume that the flow is two-dimensional, although there may be an axial velocity field that does not vary in the axial direction, and that for a typical meter we can take $R \approx 1$ cm, $\omega \approx 2500$ Hz, and $\epsilon < 10^{-2}$. We assume that the fluids are incompressible. A typical velocity is $\epsilon R \omega \approx 0.25$ m s $^{-1}$, which is much smaller than 15 m s $^{-1}$, the smallest possible sound speed in an air/water mixture at atmospheric pressure (see, for example, Ishii *et al.* 1993). We have also not considered the possibility of bubble resonance, which takes place at frequencies of the order of MHz. This problem was studied for a single fluid surrounding a rod by Retsina, Richardson & Wakeham (1986). A device based on a vibrating rod has been used for single-phase density measurement (see Bett *et al.* 1989), and the analysis given in Retsina *et al.* (1986) was used directly and in detail to help design the meter. Our objective in the present paper is somewhat different. We treat this as a model problem that will allow us to gain some insight first into whether a typical device is likely to be interpretable under any circumstances in two-phase flow, and secondly into why a simple interpretation may be inappropriate.

We shall begin by considering separated flows with two distinct regions, which we label D_1 and D_2 , where the fluid densities are ρ_1 and ρ_2 respectively. The equations for conservation of mass and momentum in each region are

$$\nabla \cdot \mathbf{u}_j = 0, \quad (2.1)$$

$$\rho_j \left(\frac{\partial \mathbf{u}_j}{\partial t} + \mathbf{u}_j \cdot \nabla \mathbf{u}_j \right) = -\nabla p_j + \mu_j \nabla^2 \mathbf{u}_j, \quad (2.2)$$

for $j = 1, 2$, where \mathbf{u}_j , p_j and μ_j are the fluid velocity, pressure and viscosity in region D_j . These are to be solved subject to the boundary conditions

$$\mathbf{u}_j = i\omega \epsilon R e^{i\omega t} \hat{\mathbf{x}} \quad \text{at } r = R \left(\epsilon e^{i\omega t} \cos \theta + (1 - \epsilon^2 e^{2i\omega t} \sin^2 \theta)^{1/2} \right), \quad (2.3)$$

where $\hat{\mathbf{x}}$ is a unit vector in the direction of oscillation, $\theta = 0$, and

$$\mathbf{u}_j = 0 \quad \text{at } r = R_C. \quad (2.4)$$

We can estimate the strength of inertial forces relative to surface tension forces by calculating the Weber number, $We = \rho \epsilon R^3 \omega^2 / \sigma$, where σ is the surface tension. Note that the radius of curvature of the surface is of $O(R/\epsilon)$ since the surface displacement is of $O(\epsilon R)$ and the lengthscale for radial disturbances is of $O(R)$. For typical air/water or oil/water mixtures, $\sigma \approx 5 \times 10^{-2} \text{ kg s}^{-2}$ and hence, using the typical values noted earlier, $We \approx 1000$. This means that typically surface tension forces are negligibly small relative to inertial forces. Note that the boundary conditions at the fluid/fluid interface can be applied at the undisturbed position of the interface, at leading order. For notational convenience, we make this approximation at the interface now, and also anticipate the result, derived below, that the flow is inviscid at leading order. Continuity of normal velocity and pressure must therefore hold at the interface, so that

$$p_1 = p_2, \quad \mathbf{u}_1 \cdot \mathbf{n} = \mathbf{u}_2 \cdot \mathbf{n} \quad \text{at } D_1 \cap D_2, \quad (2.5)$$

where \mathbf{n} is the unit normal to the fluid/fluid interface.

Appropriate dimensionless variables are

$$\hat{r} = r/R, \quad \hat{\mathbf{u}}_j = \mathbf{u}_j / \epsilon R \omega, \quad \hat{p}_j = p / \rho_j \epsilon R^2 \omega^2, \quad \hat{t} = \omega t. \quad (2.6)$$

In terms of these variables, (2.1) to (2.4) become

$$\hat{\nabla} \cdot \hat{\mathbf{u}}_j = 0, \quad (2.7)$$

$$\frac{\partial \hat{\mathbf{u}}_j}{\partial \hat{t}} + \epsilon \hat{\mathbf{u}}_j \cdot \hat{\nabla} \hat{\mathbf{u}}_j = -\hat{\nabla} \hat{p}_j + Re_j^{-1} \hat{\nabla}^2 \hat{\mathbf{u}}_j, \quad (2.8)$$

subject to

$$\hat{\mathbf{u}}_j = i e^{i\hat{t}} \hat{\mathbf{x}} \quad \text{at } \hat{r} = \epsilon e^{i\hat{t}} \cos \theta + (1 - \epsilon^2 e^{2i\hat{t}} \sin^2 \theta)^{1/2}, \quad (2.9)$$

$$\hat{\mathbf{u}}_j = 0 \quad \text{at } \hat{r} = \hat{R}_C, \quad (2.10)$$

where

$$Re_j = \rho_j \omega R^2 / \mu_j, \quad \hat{R}_C = R_C / R. \quad (2.11)$$

For the typical values quoted earlier, $Re_j \approx 2.5 \times 10^6$, and, as stated above, the flow is inviscid at leading order. As $\epsilon \rightarrow 0$ the nonlinear advection terms become small and the momentum equation (2.8) is linear at leading order. In addition, the boundary conditions at the surface of the vibrating rod can be applied at the undisturbed position. The leading-order problem is therefore

$$\frac{\partial \mathbf{u}_j}{\partial \hat{t}} = -\hat{\nabla} \hat{p}_j, \quad \hat{\nabla} \cdot \hat{\mathbf{u}}_j = 0,$$

and hence

$$\hat{\nabla}^2 \hat{p}_j = 0, \quad (2.12)$$

subject to

$$\frac{\partial \hat{p}_j}{\partial \hat{r}} = e^{i\hat{t}} \cos \theta \quad \text{at } \hat{r} = 1, \quad (2.13)$$

$$\frac{\partial \hat{p}_j}{\partial \hat{r}} = 0 \quad \text{at } \hat{r} = \hat{R}_C, \quad (2.14)$$

$$\hat{\rho} \hat{p}_1 = \hat{p}_2, \quad \mathbf{n} \cdot \hat{\nabla} \hat{p}_1 = \mathbf{n} \cdot \hat{\nabla} \hat{p}_2 \quad \text{at } D_1 \cap D_2, \quad (2.15)$$

where $\hat{\rho} = \rho_1/\rho_2$. For this inviscid problem we can only apply boundary conditions on the normal components of the velocity at the solid surfaces. The boundary conditions that govern the transverse velocity components at the solid surfaces are satisfied across boundary layers. Note that the axial velocity distribution does not appear in the problem that governs the transverse velocity components.

If we apply Newton's second law to the vibrating rod we find that

$$F = -\epsilon R \omega^2 (m_f + m_0) e^{i\omega t}, \quad (2.16)$$

where F is the force on the rod, m_f is the added mass contributed by the surrounding fluid, and m_0 is the mass of the rod, all per unit length. *In vacuo*, the force required to drive the oscillation is $F_0 = -\epsilon R \omega^2 m_0 e^{i\omega t}$. When the rod is surrounded by fluid, the added mass contribution, $-\epsilon R \omega^2 m_f e^{i\omega t}$, must come from the force exerted by the fluid on the rod. At leading order therefore, the added mass provided by the fluid is given by

$$m_f = -\frac{R^2}{e^{i\omega t}} \int_0^{2\pi} \rho_j \hat{p}_j|_{\hat{r}=1} \cos \theta d\theta. \quad (2.17)$$

Note that viscous drag is negligible at leading order and moreover the correction term is imaginary. This leads to a contribution to the drag that is out of phase with the force due to added mass by 90° and can easily be removed by signal processing. The leading-order contribution from the viscous force on the rod that is in phase with the added mass force is therefore even smaller, of $O(Re_f^{-2})$.

In a real meter the vibrating element has a finite length and a well-defined resonant frequency. In practice it is this resonant frequency that is measured. However, a measurement of the resonant frequency is used to determine the added mass provided by the surrounding fluid, as described in Retsina *et al.* (1986). The resonant frequency of a different type of vibrating element, a flat plate, is analysed in detail for the case of a single fluid in Cumberbatch & Wilks (1987). This is also shown to be related to the added mass of the fluid accelerated during the vibration. We shall proceed on the basis that the measurement made is effectively of the added mass of the fluid.

3. Single-phase solution

When only one fluid is present outside the rod we must simply solve Laplace's equation (2.12) subject to the boundary conditions (2.13) and (2.14). The solution is

$$\hat{p} = \frac{e^{i\hat{t}}}{1 - \hat{R}_C^2} \left(\hat{r} + \frac{\hat{R}_C^2}{\hat{r}} \right) \cos \theta, \quad (3.1)$$

and hence

$$m_f = \frac{\hat{R}_C^2 + 1}{\hat{R}_C^2 - 1} \rho_1 \pi R^2. \quad (3.2)$$

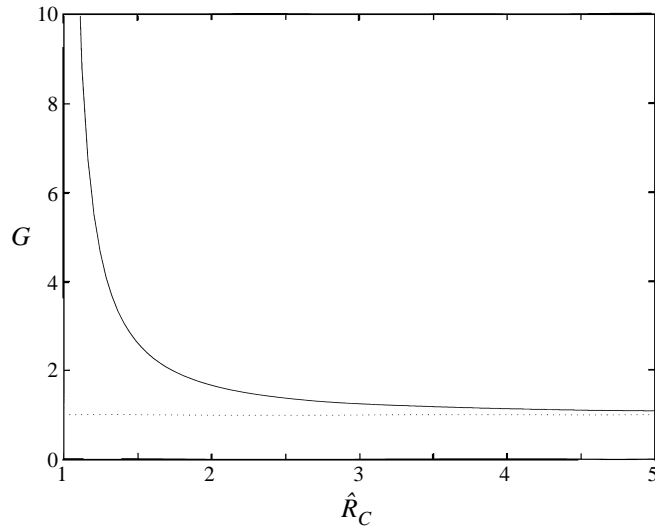


FIGURE 2. The geometrical factor, $G(\hat{R}_C)$, plotted as a function of $\hat{R}_C = R_C/R$. The dotted line is the asymptote, $G = 1$.

In this case the added mass is simply the mass displaced by the rod, $\rho_1\pi R^2$, multiplied by a geometrical factor that tends to unity as $\hat{R}_C \rightarrow \infty$. This geometrical factor, $G(\hat{R}_C)$, defined as

$$G(\hat{R}_C) = \frac{\hat{R}_C^2 + 1}{\hat{R}_C^2 - 1} = \frac{R_C^2 + R^2}{R_C^2 - R^2}, \tag{3.3}$$

tells us about the effect of the rigid pipe wall at $r = R_C$, and is plotted in figure 2. There are two ways of thinking about this. First, if the effect of the pipe wall is neglected we can ask what is the error in the calculation of the fluid density. For $\hat{R}_C^2 \gg 1$, $G \sim 1 + 2/\hat{R}_C^2$, so for an error of less than 1% we require $\hat{R}_C > \sqrt{200} \approx 14.1$. This is consistent with the conclusions reached by a more circuitous route in Retsina *et al.* (1986), where figure 4 shows an equivalent result. Secondly, if we want the meter to be affected by the density across as much of the pipe as possible the pipe wall should not be so far away that its effect can be neglected, since then there is some part of the fluid in the neighbourhood of the pipe wall whose density is not being measured. Only the first consideration is relevant to single-phase flow, where the density is uniform. Figure 2 shows the decreasing effect of the pipe wall on the measurement as \hat{R}_C increases. This indicates that the measurement is perhaps rather more localized than we would like if the distribution of the fluid density is not uniform. We investigate this further in the following section.

Finally, note that (3.2) shows that the added mass is directly proportional to the fluid density. In the following analysis, where two fluids are present outside the rod, the simplest interpretation of the measured added mass is to assume an effectively single-phase mixture, so that the dimensionless inferred density, $\hat{\rho}_{meas} = \rho_{meas}/\rho_2$, is given by

$$\hat{\rho}_{meas} = \frac{\hat{R}_C^2 - 1}{\hat{R}_C^2 + 1} \frac{m_f}{\rho_2\pi R^2}. \tag{3.4}$$

4. Concentric layers

In order to investigate how our simplified device responds to different densities of fluid at different distances from the rod we consider the behaviour in two concentric layers of different fluids. The interface between the fluids lies at $R = R_I$, with fluid 1 nearest the rod. The solution of (2.12) that satisfies the boundary conditions (2.13) to (2.15) is of the same form as that for a single fluid, with

$$\hat{p}_j = e^{i\hat{t}} \cos \theta (A_j \hat{r} + B_j / \hat{r}), \quad (4.1)$$

where

$$A_1 = \frac{\hat{\rho} (\hat{R}_C^2 - \hat{R}_I^2) - (\hat{R}_C^2 + \hat{R}_I^2)}{\hat{\rho} (\hat{R}_C^2 - \hat{R}_I^2) (\hat{R}_I^2 + 1) + (\hat{R}_C^2 + \hat{R}_I^2) (\hat{R}_I^2 - 1)}, \quad (4.2a)$$

$$B_1 = \frac{-\hat{R}_I^2 \{ \hat{\rho} (\hat{R}_C^2 - \hat{R}_I^2) + (\hat{R}_C^2 + \hat{R}_I^2) \}}{\hat{\rho} (\hat{R}_C^2 - \hat{R}_I^2) (\hat{R}_I^2 + 1) + (\hat{R}_C^2 + \hat{R}_I^2) (\hat{R}_I^2 - 1)}, \quad (4.2b)$$

$$A_2 = -\frac{2\hat{\rho}\hat{R}_I^2}{\hat{\rho} (\hat{R}_C^2 - \hat{R}_I^2) (\hat{R}_I^2 + 1) + (\hat{R}_C^2 + \hat{R}_I^2) (\hat{R}_I^2 - 1)}, \quad (4.2c)$$

$$B_2 = -\frac{2\hat{\rho}\hat{R}_C^2\hat{R}_I^2}{\hat{\rho} (\hat{R}_C^2 - \hat{R}_I^2) (\hat{R}_I^2 + 1) + (\hat{R}_C^2 + \hat{R}_I^2) (\hat{R}_I^2 - 1)}. \quad (4.2d)$$

From this we find that

$$m_f = \frac{\hat{\rho} (\hat{R}_C^2 - \hat{R}_I^2) (\hat{R}_I^2 - 1) + (\hat{R}_C^2 + \hat{R}_I^2) (\hat{R}_I^2 + 1)}{\hat{\rho} (\hat{R}_C^2 - \hat{R}_I^2) (\hat{R}_I^2 + 1) + (\hat{R}_C^2 + \hat{R}_I^2) (\hat{R}_I^2 - 1)} \rho_1 \pi R^2, \quad (4.3)$$

and hence that

$$\hat{\rho}_{meas} = \hat{\rho} \left(\frac{\hat{R}_C^2 - 1}{\hat{R}_C^2 + 1} \right) \frac{\hat{\rho} (\hat{R}_C^2 - \hat{R}_I^2) (\hat{R}_I^2 - 1) + (\hat{R}_C^2 + \hat{R}_I^2) (\hat{R}_I^2 + 1)}{\hat{\rho} (\hat{R}_C^2 - \hat{R}_I^2) (\hat{R}_I^2 + 1) + (\hat{R}_C^2 + \hat{R}_I^2) (\hat{R}_I^2 - 1)}. \quad (4.4)$$

When $\hat{R}_C \gg 1$ with $\hat{R}_I = O(1)$, the wall of the pipe is far from the rod, and we can consider the effect on the measured density of the size of the layer of fluid on the rod. This is illustrated in figures 3(a) and 3(b). As the layer thickness increases the measured density changes from that of fluid 2 to that of fluid 1, as expected. When $\hat{\rho} \ll 1$ the layer on the rod has a much lower density than the bulk fluid. In this case the measured density rapidly approaches that of the fluid layer, with $\hat{\rho}_{meas} = O(\hat{\rho})$ when $\hat{R}_I = O(\hat{\rho})$, as illustrated in figure 3(a). In other words, a thin coating of low-density fluid can mask the presence of the outer, higher-density fluid. This is clearly to be avoided in practice, if at all possible. In the opposite case, $\hat{\rho} \gg 1$, the change in measured density is more gradual, and $\hat{\rho}_{meas}$ increases on an $O(1)$ lengthscale, independent of the magnitude of $\hat{\rho}$, as illustrated in figure 3(b).

In general, we can write the measured fraction of fluid 1, α_{meas} , in terms of the measured density by noting that

$$\alpha_{meas} = (\hat{\rho}_{meas} - 1) / (\hat{\rho} - 1), \quad (4.5)$$

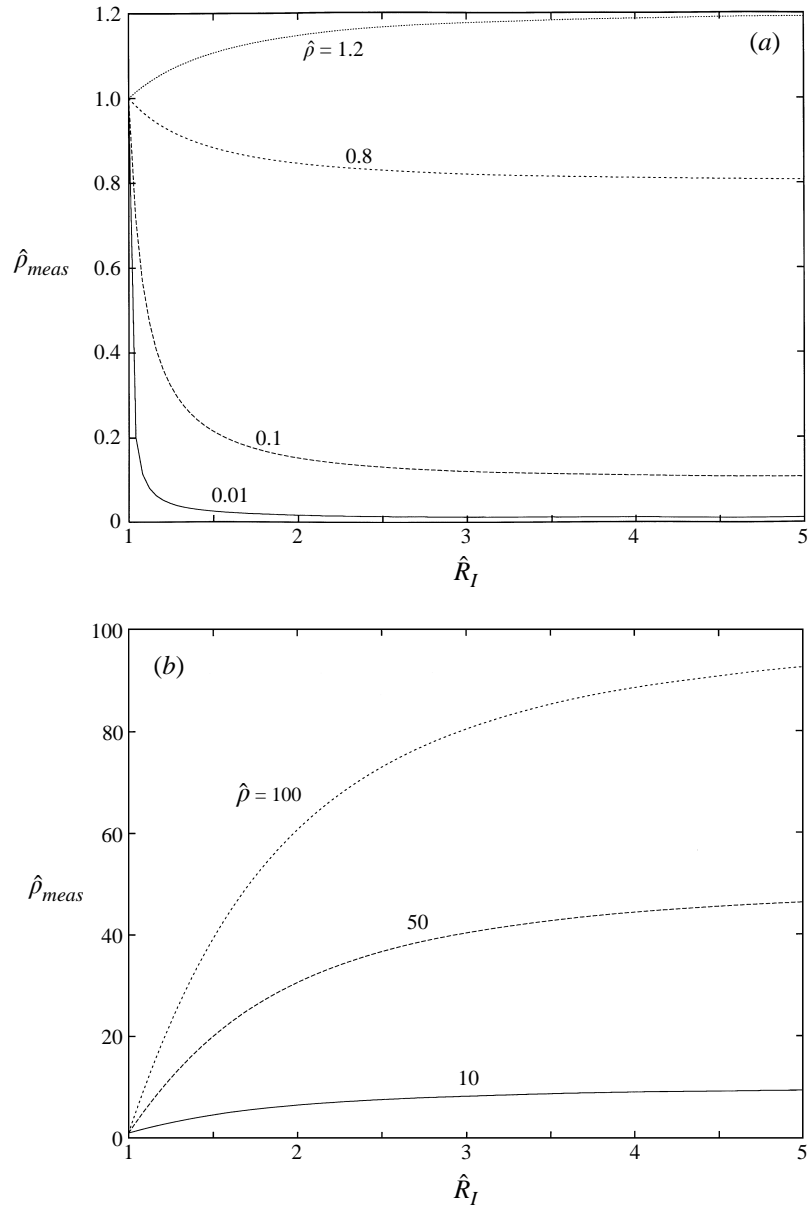


FIGURE 3. The dimensionless measured density, $\hat{\rho}_{meas}$, plotted as a function of the dimensionless inner layer thickness, \hat{R}_I , when the wall of the pipe is far from the rod ($\hat{R}_C \gg 1$), for density ratios (a) $\hat{\rho} = 0.01, 0.1, 0.8, 1.2$; (b) $\hat{\rho} = 10, 50, 100$.

and hence that for concentric layers

$$\alpha_{meas} = \frac{\hat{R}_I^2 - 1}{\hat{R}_C^2 + 1} \frac{\hat{\rho}^2 (\hat{R}_C^2 - 1) (\hat{R}_C^2 - \hat{R}_I^2) + 2\hat{\rho}\hat{R}_C^2 (\hat{R}_I^2 + 1) - (\hat{R}_C^2 + 1) (\hat{R}_C^2 + \hat{R}_I^2)}{(\hat{\rho} - 1) \{ \hat{\rho} (\hat{R}_C^2 - \hat{R}_I^2) (\hat{R}_I^2 + 1) + (\hat{R}_C^2 + \hat{R}_I^2) (\hat{R}_I^2 - 1) \}}. \quad (4.6)$$

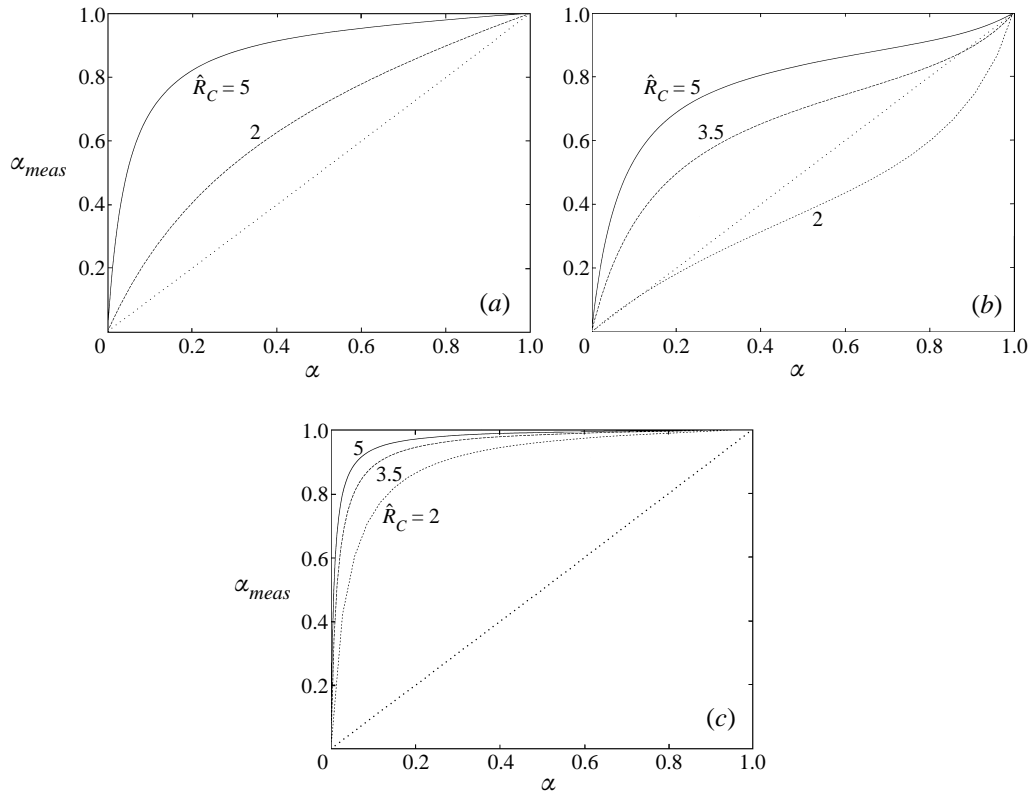


FIGURE 4. The measured fraction of fluid 1 plotted against the actual fraction for (a) $\hat{\rho} = 1.2$ and $\hat{R}_C = 2, 5$; (b) $\hat{\rho} = 10$ and $\hat{R}_C = 2, 3.5, 5$; (c) $\hat{\rho} = 0.1$ and $\hat{R}_C = 2, 3.5, 5$. The dotted line is $\alpha_{meas} = \alpha$.

The actual value of, α , the fraction of fluid 1 is

$$\alpha = \frac{\hat{R}_I^2 - 1}{\hat{R}_C^2 - 1}. \quad (4.7)$$

Figure 4 shows plots of α_{meas} against α for various values of $\hat{\rho}$ and \hat{R}_C . In figure 4(a), $\hat{\rho} = 1.2$, which is a typical value for a layer of water surrounded by a layer of oil. It is clear that the simple, single-phase interpretation is not correct in this case, with the interpretation becoming worse as \hat{R}_C increases. This is not really surprising, since this type of separated flow is the most unfavourable arrangement of fluid for this simple interpretation. If we could guarantee that the fluids would be arranged in concentric layers, (4.6) would allow us to interpret the response of the device. Figure 4(b) shows the response when the fluid density contrast is somewhat greater, perhaps for a layer of water surrounded by gas in a high-pressure environment. Figure 4(c) shows what happens when the fluid on the rod has a much lower density than the other fluid. As we would expect from the results shown in figure 3(a), a small actual fraction of low-density fluid on the rod is enough to make the device respond as if it were almost entirely surrounded by it.

The above analysis has shown us what happens when the fluids have a radially stratified arrangement. We now consider the response of the device in a circumferentially stratified medium.

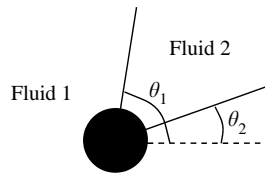


FIGURE 5. The arrangement of the circumferentially stratified fluids.

5. Circumferentially stratified fluids

Ideally, we would like to study the response of the device when the fluids exist as two regions separated by radii of the pipe cross-section. Unfortunately there is no analytical solution available for this geometry. However we can develop an analytical solution in the limit $\hat{R}_C = \infty$ with two fluids separated by radii running from $\hat{r} = 1$ to infinity. This idealized situation will give us some idea of the dependence of the response on the circumferential position of the two fluids. We have already studied the dependence on the position of the pipe wall and the radial position of the fluids, so it is not unreasonable to study this case with the pipe wall far from the rod.

The full problem that we wish to solve, dropping the hats for notational convenience, is now

$$\nabla^2 p_j = 0, \tag{5.1}$$

for $r \geq 1$, $\theta_2 \leq \theta < \theta_2 + 2\pi$, subject to

$$\frac{\partial p_j}{\partial r} = e^{it} \cos \theta \quad \text{at } r = 1, \tag{5.2}$$

$$p_j \rightarrow 0 \quad \text{as } r \rightarrow \infty, \tag{5.3}$$

$$\hat{\rho} p_1 = p_2, \quad \frac{\partial p_1}{\partial \theta} = \frac{\partial p_2}{\partial \theta} \quad \text{at } \theta = \theta_1 \text{ and } \theta = \theta_2, \tag{5.4}$$

where fluid 2 lies in the sector $\theta_2 \leq \theta \leq \theta_1$ and fluid 1 lies in the sector $\theta_1 \leq \theta \leq \theta_2 + 2\pi$, as shown in figure 5.

We can solve the boundary value problem defined by (5.1) to (5.4) using finite Mellin transforms (see Sneddon 1973). We define the finite Mellin transform, $P_j(s, \theta)$, of $p_j(r, \theta)$ as

$$P_j(s, \theta) = \int_1^\infty \left(\frac{1}{r^{s+1}} + r^{s-1} \right) p_j(r, \theta) dr. \tag{5.5}$$

Finite Mellin transforms are most often used to solve boundary value problems in finite sectors that include the origin, in which case the integral ranges from zero to one, hence the name. Using the transformation $r \mapsto 1/r$, the integral transform given by (5.5) is obtained, although 'finite' is now something of a misnomer. If $p_j(r, \theta) = O(r^{-k_j})$ as $r \rightarrow \infty$, then $P_j(s, \theta)$ is analytic in the strip $-k_j < \text{Re}(s) < k_j$. By seeking a far-field solution of the form

$$p_j(r, \theta) \sim r^{-k_j} \{ C_j \sin(k_j \theta) + D_j \cos(k_j \theta) \}, \tag{5.6}$$

that satisfies the four boundary conditions given by (5.4), we find that $k_1 = k_2 = k$, and that k must satisfy the solvability condition

$$F(k) \equiv -4\hat{\rho} + (1 + \hat{\rho})^2 \cos(2\pi k) - (1 - \hat{\rho})^2 \cos\{2k(-\pi + \theta_1 - \theta_2)\} = 0. \tag{5.7}$$

We therefore require P_j to be analytic in the strip $-k_0 < \text{Re}(s) < k_0$, where k_0 is the smallest positive root of (5.7).

The finite Mellin transform of (5.1) subject to the boundary condition (5.2) is

$$\frac{\partial^2 P_j}{\partial \theta^2} + s^2 P_j = -2e^{it} \cos \theta. \quad (5.8)$$

Note that in order to make this simplification of the Laplacian we require that $(r^{-s} + r^s)r\hat{\partial}p_j/\partial r \rightarrow 0$ as $r \rightarrow \infty$. This excludes the possibility of a logarithmic singularity in p_j as $r \rightarrow \infty$. Equation (5.8) has the general solution

$$P_j = A_j(s) \sin(s\theta) + B_j(s) \cos(s\theta) - \frac{2e^{it} \cos \theta}{s^2 - 1}. \quad (5.9)$$

In order to determine the functions $A_j(s)$ and $B_j(s)$ we must apply the continuity conditions (5.4). We find that

$$\hat{\rho}A_1 \sin(s\theta_1) + \hat{\rho}B_1 \cos(s\theta_1) - A_2 \sin(s\theta_1) - B_2 \cos(s\theta_1) = \frac{2(\hat{\rho} - 1)e^{it} \cos \theta_1}{s^2 - 1}, \quad (5.10)$$

$$\begin{aligned} \hat{\rho}A_1 \sin\{s(\theta_2 + 2\pi)\} + \hat{\rho}B_1 \cos\{s(\theta_2 + 2\pi)\} - A_2 \sin(s\theta_2) - B_2 \cos(s\theta_2) \\ = \frac{2(\hat{\rho} - 1)e^{it} \cos \theta_2}{s^2 - 1}, \end{aligned} \quad (5.11)$$

$$A_1 \cos(s\theta_1) - B_1 \sin(s\theta_1) - A_2 \cos(s\theta_1) + B_2 \sin(s\theta_1) = 0, \quad (5.12)$$

$$A_1 \cos\{s(\theta_2 + 2\pi)\} - B_1 \sin\{s(\theta_2 + 2\pi)\} - A_2 \cos(s\theta_2) + B_2 \sin(s\theta_2) = 0. \quad (5.13)$$

The solution of these linear equations can be written in the form $A_j = a_j e^{it}/K$ and $B_j = b_j e^{it}/K$, where

$$\begin{aligned} a_1 = \cos \theta_1 [-(1 - \hat{\rho}) \sin\{s(-2\pi + \theta_1 - 2\theta_2)\} \\ + (1 + \hat{\rho}) \sin\{s(2\pi + \theta_1)\} - 2 \sin(s\theta_1)] \\ + \cos \theta_2 [(1 - \hat{\rho}) \sin\{s(2\theta_1 - \theta_2)\} \\ + (1 + \hat{\rho}) \sin(s\theta_2) - 2 \sin\{s(2\pi + \theta_2)\}], \end{aligned} \quad (5.14)$$

$$\begin{aligned} b_1 = \cos \theta_1 [(1 - \hat{\rho}) \cos\{s(-2\pi + \theta_1 - 2\theta_2)\} \\ + (1 + \hat{\rho}) \cos\{s(2\pi + \theta_1)\} - 2 \cos(s\theta_1)] \\ + \cos \theta_2 [(1 - \hat{\rho}) \cos\{s(2\theta_1 - \theta_2)\} \\ + (1 + \hat{\rho}) \cos(s\theta_2) - 2 \cos\{s(2\pi + \theta_2)\}], \end{aligned} \quad (5.15)$$

$$\begin{aligned} a_2 = -\cos \theta_1 [(1 - \hat{\rho}) \sin\{s(-2\pi + \theta_1 - 2\theta_2)\} \\ + (1 + \hat{\rho}) \sin\{s(-2\pi + \theta_1)\} - 2\hat{\rho} \sin(s\theta_1)] \\ - \cos \theta_2 [-(1 - \hat{\rho}) \sin\{s(-2\pi + 2\theta_1 - \theta_2)\} \\ + (1 + \hat{\rho}) \sin\{s(2\pi + \theta_2)\} - 2\hat{\rho} \sin(s\theta_2)] \end{aligned} \quad (5.16)$$

$$\begin{aligned} b_2 = -\cos \theta_1 [-(1 - \hat{\rho}) \cos\{s(-2\pi + \theta_1 - 2\theta_2)\} \\ + (1 + \hat{\rho}) \cos\{s(-2\pi + \theta_1)\} - 2\hat{\rho} \cos(s\theta_1)] \\ - \cos \theta_2 [-(1 - \hat{\rho}) \cos\{s(-2\pi + 2\theta_1 - \theta_2)\} \\ + (1 + \hat{\rho}) \cos\{s(2\pi + \theta_2)\} - 2\hat{\rho} \cos(s\theta_2)], \end{aligned} \quad (5.17)$$

$$K = (s^2 - 1) F(s) / 2(\hat{\rho} - 1). \quad (5.18)$$

It is now clear that the solutions, P_j , have poles at the roots of $F(s) = 0$, as expected.

Although it appears that there are two other poles at $s = \pm 1$, these zeros in $F(s)$ are balanced by zeros in the numerators, and the functions $P_j(s, \theta)$ are analytic in the strip $-k_0 < \text{Re}(s) < k_0$, as required. The Mellin inversion formula can now be written as

$$p_j(r, \theta) = -\frac{1}{2\pi i} \int_{-i\infty}^{i\infty} r^s P_j(s, \theta) ds. \tag{5.19}$$

This allows us to write down the measured density, $\hat{\rho}_{meas}$, using (2.17) and (3.4), as

$$\begin{aligned} \hat{\rho}_{meas} = & -\frac{1}{2\pi^2 i} \int_{-i\infty}^{i\infty} \left[\frac{2}{s^2 - 1} \left\{ \int_{\theta_2}^{\theta_1} \cos^2 \theta d\theta + \hat{\rho} \int_{\theta_1}^{\theta_2+2\pi} \cos^2 \theta d\theta \right\} \right. \\ & - A_2(s) \int_{\theta_2}^{\theta_1} \sin(s\theta) \cos \theta d\theta - \hat{\rho} A_1(s) \int_{\theta_1}^{\theta_2+2\pi} \sin(s\theta) \cos \theta d\theta \\ & \left. - B_2(s) \int_{\theta_2}^{\theta_1} \cos(s\theta) \cos \theta d\theta - \hat{\rho} B_1(s) \int_{\theta_1}^{\theta_2+2\pi} \cos(s\theta) \cos \theta d\theta \right] ds. \tag{5.20} \end{aligned}$$

The expression in curly brackets can be integrated with respect to θ immediately, and then integrated with respect to s by closing the contour in the left half-plane and evaluating the residue at $s = -1$. Finally, after evaluating the remaining θ integrals and simplifying as far as possible using (5.15) to (5.18), we find that, in terms of the measured and actual fractions of fluid 1,

$$\begin{aligned} \alpha_{meas} = & \alpha - \frac{2(1 - \hat{\rho})}{2\pi^2 i} (\cos^2 \theta_1 + \cos^2 \theta_2) \\ & \times \int_{-i\infty}^{i\infty} \frac{s [(1 + \hat{\rho}) \sin(2\pi s) - (1 - \hat{\rho}) \sin\{2\pi s(1 - 2\alpha)\}]}{(1 - s^2)^2 [-4\hat{\rho} + (1 + \hat{\rho})^2 \cos(2\pi s) - (1 - \hat{\rho})^2 \cos\{2\pi s(1 - 2\alpha)\}]} ds \\ & + \frac{8(1 - \hat{\rho})}{2\pi^2 i} \cos \theta_1 \cos \theta_2 \\ & \times \int_{-i\infty}^{i\infty} \frac{s [\hat{\rho} \sin\{2\pi s(1 - \alpha)\} + \sin(2\pi s\alpha)]}{(1 - s^2)^2 [-4\hat{\rho} + (1 + \hat{\rho})^2 \cos(2\pi s) - (1 - \hat{\rho})^2 \cos\{2\pi s(1 - 2\alpha)\}]} ds. \tag{5.21} \end{aligned}$$

We can see immediately that for $|\hat{\rho} - 1| \ll 1$ the measured fraction is correct at leading order, but that there will be a significant error otherwise. For the special case, $\theta_1 - \theta_2 = \pi$, when there are equal amounts of each fluid, we can evaluate the integrals in (5.21) analytically. First we note that in this case

$$\alpha_{meas} = \alpha - \frac{4(\hat{\rho} - 1)^2}{2\pi^2 i (1 + \hat{\rho})} \cos^2 \theta_2 \int_{-i\infty}^{i\infty} \frac{s \cot(\pi s/2)}{(1 - s^2)^2} ds. \tag{5.22}$$

The integrand has simple poles on the real axis at $s = \pm 1$ and $s = \pm 2n$, with $n = 1, 2, \dots$. Note that the poles at $s = \pm 1$ were introduced by the integration around the vibrating rod and are not present in the transformed pressures, P_j . In this case we can readily calculate the integral by closing the contour of integration in the left half-plane and summing the residues at the enclosed poles. We find that

$$\frac{1}{2\pi i} \int_{-i\infty}^{i\infty} \frac{s \cot(\pi s/2)}{(1 - s^2)^2} ds = \frac{\pi}{8} - \frac{1}{\pi} \sum_{n=1}^{\infty} \frac{4n}{(1 - 4n^2)^2}. \tag{5.23}$$

The infinite sum in this expression becomes trivial when decomposed into partial

fractions, and we finally obtain

$$\alpha_{meas} = \frac{1}{2} + \frac{(1 - \hat{\rho})}{2(1 + \hat{\rho})} \left(1 - \frac{4}{\pi^2}\right) \cos^2 \theta_2. \quad (5.24)$$

Clearly, the measured fraction of fluid 1 is correct when $\theta_2 = \pi/2$ or $3\pi/2$, when the rod vibrates at right angles to the interface. In each of these cases the exact solution for the pressure field in each fluid is $p_j = -e^{it} \cos \theta/r$, the same as the single-phase solution. We can also see that the error is greatest when $\theta_2 = 0$ or π , when the rod vibrates in the direction of the interface. In the worst possible case, with $\hat{\rho} = 0$ or ∞ and $\theta_2 = 0$ or π , $\alpha_{meas} \approx 0.5 \pm 0.297$.

In general, we must evaluate the integrals in (5.21) numerically. We can write (5.21) in terms of integrals on the real line as

$$\begin{aligned} \alpha_{meas} = & \alpha + \frac{2(1 - \hat{\rho})}{\pi^2} (\cos^2 \theta_1 + \cos^2 \theta_2) \\ & \times \int_0^\infty \frac{u [(1 + \hat{\rho}) \sinh(2\pi u) - (1 - \hat{\rho}) \sinh\{2\pi u(1 - 2\alpha)\}]}{(1 + u^2)^2 [-4\hat{\rho} + (1 + \hat{\rho})^2 \cosh(2\pi u) - (1 - \hat{\rho})^2 \cosh\{2\pi u(1 - 2\alpha)\}]} du \\ & - \frac{8(1 - \hat{\rho})}{\pi^2} \cos \theta_1 \cos \theta_2 \\ & \times \int_0^\infty \frac{u [\hat{\rho} \sinh\{2\pi u(1 - \alpha)\} + \sinh(2\pi u\alpha)]}{(1 + u^2)^2 [-4\hat{\rho} + (1 + \hat{\rho})^2 \cosh(2\pi u) - (1 - \hat{\rho})^2 \cosh\{2\pi u(1 - 2\alpha)\}]} du. \end{aligned} \quad (5.25)$$

The integrands in (5.25) decay exponentially fast as $u \rightarrow \infty$ and the integrals are easy to evaluate numerically using the trapezium rule. We can use (5.24) for the special case $\theta_1 - \theta_2 = \pi$ to verify that this numerical evaluation of the integrals is correct.

Figures 6(a) and 6(b) show that when the fluid densities are comparable the measured fluids fractions are close to the actual values. We must note, however, that (4.5) shows that in this case α_{meas} is defined as the ratio of two small quantities. This means that, although in theory the device works well, small errors inherent in the measurement process may be amplified in this case. Figures 6(c) and 6(d) show that this is not the case when there is a significant density contrast between the fluids. The measured values of α vary enormously depending on the orientation of the sectors for a given liquid fraction and, unless $\alpha = 0.5$, the measured fraction is never close to the actual fraction.

6. A multiphase mixture

The final case that we consider is of a multiphase mixture that consists of a continuous phase, which we label as fluid 1, and a dispersed phase, labelled as fluid 2. We shall make the usual continuum approximation for such a mixture, and use α to represent the local fraction of the continuous phase. The approximation procedure is described in Drew (1983). The relevant governing equations are

$$\nabla \cdot \{\alpha \mathbf{u}_1 + (1 - \alpha) \mathbf{u}_2\} = 0, \quad (6.1)$$

$$\rho_1 \alpha \left(\frac{\partial \mathbf{u}_1}{\partial t} + \mathbf{u}_1 \cdot \nabla \mathbf{u}_1 \right) = -\alpha \nabla p + \mu_1 \alpha \nabla^2 \mathbf{u}_1 - \mathbf{D} - \mathbf{A}, \quad (6.2)$$

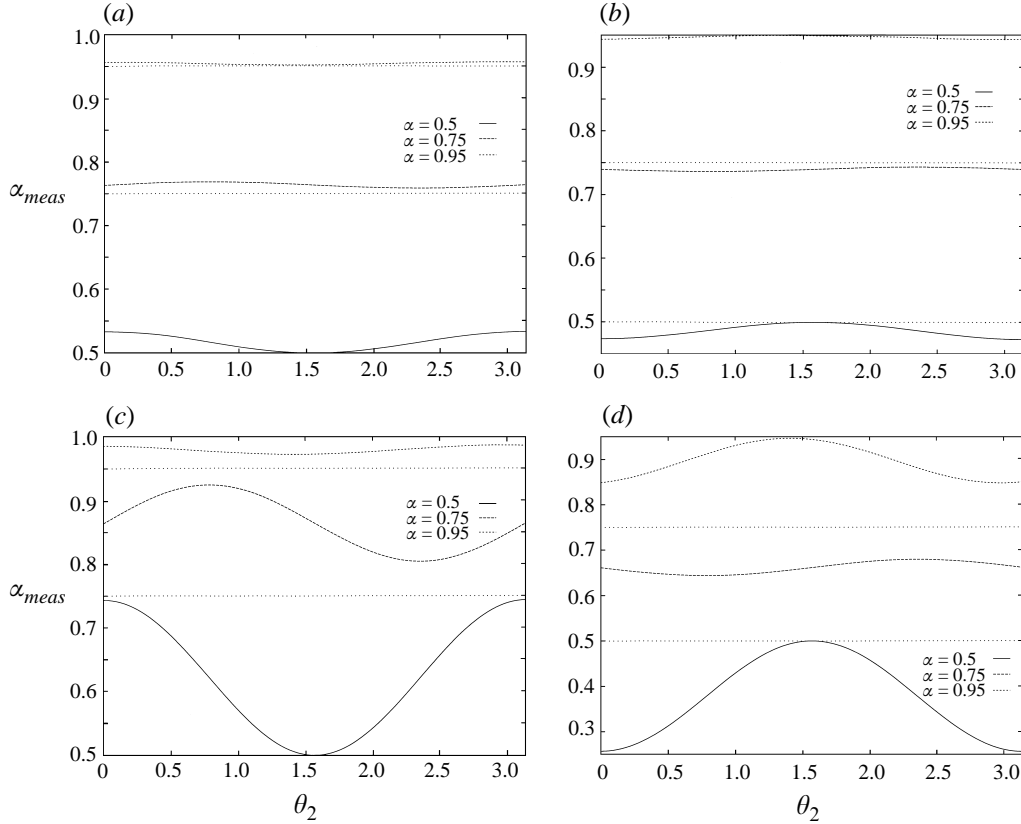


FIGURE 6. The fraction of fluid 1 measured by the device when the fluids are circumferentially stratified with (a) $\hat{\rho} = 0.8$, (b) $\hat{\rho} = 1.2$, (c) $\hat{\rho} = 0.1$, (d) $\hat{\rho} = 10$.

$$\rho_2(1-\alpha) \left(\frac{\partial \mathbf{u}_2}{\partial t} + \mathbf{u}_2 \cdot \nabla \mathbf{u}_2 \right) = -(1-\alpha) \nabla p + \mu_2(1-\alpha) \nabla^2 \mathbf{u}_2 + \mathbf{D} + \mathbf{A}, \quad (6.3)$$

where

$$\mathbf{D} = \frac{-12\pi\mu_1 R_b(1-\alpha)(\mathbf{u}_2 - \mathbf{u}_1)}{V_b}, \quad (6.4)$$

$$\mathbf{A} = -\frac{1}{2} \{ \alpha\rho_1 + (1-\alpha)\rho_2 \} \alpha(1-\alpha) \left(\frac{\partial \mathbf{u}_2}{\partial t} + \mathbf{u}_2 \cdot \nabla \mathbf{u}_2 - \frac{\partial \mathbf{u}_1}{\partial t} - \mathbf{u}_1 \cdot \nabla \mathbf{u}_1 \right), \quad (6.5)$$

subject to

$$\mathbf{u}_1 = \mathbf{u}_2 = 0 \quad \text{at } r = R_C, \quad (6.6)$$

$$\mathbf{u}_1 = \mathbf{u}_2 = i\omega\epsilon R e^{i\omega t} \hat{\mathbf{x}} \quad \text{at } r = R \left(\epsilon e^{i\omega t} \cos \theta + (1 - \epsilon^2 e^{2i\omega t} \sin^2 \theta)^{1/2} \right). \quad (6.7)$$

Note that we have assumed that the pressure in each of the two fluid phases is equal. For dispersed flows, the difference in pressure is proportional to $|\mathbf{u}_2 - \mathbf{u}_1|^2$ (see, for example, Pauchon & Banerjee 1986). We shall see below that quadratic velocity terms do not appear at leading order in our approximation, so for ease of presentation we have assumed equal pressures from the outset.

The Stokes drag on the dispersed phase is given by \mathbf{D} , where R_b is the bubble radius and V_b the bubble volume. We have assumed that fluid 2 is monodisperse. The added mass force is given by \mathbf{A} . This represents the force that is exerted by

the fluids on each other when there is a relative acceleration. There is some debate about the appropriate form for the spatial derivatives in this force law, as described in Ishii *et al.* (1993). We have chosen what appears to be the correct form, but, as we shall see below, in the low-amplitude approximation that we shall make, all of the possible choices are equivalent at leading order. The term that multiplies the difference in fluid accelerations in definition (6.5) approaches $-\rho_1(1-\alpha)/2$ as $\alpha \rightarrow 1$, which is appropriate when fluid 2 exists as dilute spherical bubbles, and similarly as $\alpha \rightarrow 0$. When α is not close to unity this term reflects the fact that each droplet or bubble of the dispersed phase exists in a mixture with density $\alpha\rho_1 + (1-\alpha)\rho_2$.

Appropriate dimensionless variables are, as before, given by (2.6), but now with

$$\hat{p} = p/\rho_1\epsilon R^2\omega^2. \quad (6.8)$$

Equations (6.1) to (6.7) become

$$\hat{\nabla} \cdot \{\alpha\hat{\mathbf{u}}_1 + (1-\alpha)\hat{\mathbf{u}}_2\} = 0, \quad (6.9)$$

$$\alpha \left(\frac{\partial \hat{\mathbf{u}}_1}{\partial \hat{t}} + \epsilon \hat{\mathbf{u}}_1 \cdot \hat{\nabla} \hat{\mathbf{u}}_1 \right) = -\alpha \hat{\nabla} \hat{p} + Re_1^{-1} \hat{\nabla}^2 \hat{\mathbf{u}}_1 + Re_b^{-1} (1-\alpha) (\hat{\mathbf{u}}_2 - \hat{\mathbf{u}}_1) - \frac{1}{\hat{\rho}} \hat{\mathbf{A}}, \quad (6.10)$$

$$(1-\alpha) \left(\frac{\partial \hat{\mathbf{u}}_2}{\partial \hat{t}} + \epsilon \hat{\mathbf{u}}_2 \cdot \hat{\nabla} \hat{\mathbf{u}}_2 \right) = -\hat{\rho} (1-\alpha) \hat{\nabla} \hat{p} + Re_2^{-1} (1-\alpha) \hat{\nabla}^2 \hat{\mathbf{u}}_2 - \hat{\rho} Re_b^{-1} (1-\alpha) (\hat{\mathbf{u}}_2 - \hat{\mathbf{u}}_1) + \hat{\mathbf{A}}, \quad (6.11)$$

where

$$\hat{\mathbf{A}} = -\frac{1}{2} \{\alpha + \hat{\rho}(1-\alpha)\} \alpha (1-\alpha) \left(\frac{\partial \hat{\mathbf{u}}_2}{\partial \hat{t}} + \epsilon \hat{\mathbf{u}}_2 \cdot \hat{\nabla} \hat{\mathbf{u}}_2 - \frac{\partial \hat{\mathbf{u}}_1}{\partial \hat{t}} - \epsilon \hat{\mathbf{u}}_1 \cdot \hat{\nabla} \hat{\mathbf{u}}_1 \right), \quad (6.12)$$

subject to

$$\hat{\mathbf{u}}_1 = \hat{\mathbf{u}}_2 = 0 \quad \text{at } \hat{r} = \hat{R}_C, \quad (6.13)$$

$$\hat{\mathbf{u}}_1 = \hat{\mathbf{u}}_2 = ie^{i\hat{t}} \hat{\mathbf{x}} \quad \text{at } \hat{r} = \epsilon e^{i\hat{t}} \cos \theta + (1 - \epsilon^2 e^{2i\hat{t}} \sin^2 \theta)^{1/2}. \quad (6.14)$$

The dispersed-phase Reynolds number is given by

$$Re_b = \rho_1 \omega R_b^2 / 9\mu_1, \quad (6.15)$$

for spherical bubbles. For the smallest bubbles likely to be encountered, $R_b \approx 1$ mm, and hence $Re_b \approx 28$. The value of Re_b will be larger for larger bubbles. As we noted earlier, the first in-phase viscous correction to the leading-order value of the force on the rod is of $O(Re_b^{-2})$, so we shall assume that the interphase drag is negligibly small, with $Re_b \gg 1$.

At leading order for $Re_j \gg 1$, $Re_b \gg 1$ and $\epsilon \ll 1$

$$\alpha \frac{\partial \hat{\mathbf{u}}_1}{\partial \hat{t}} = -\alpha \hat{\nabla} \hat{p} + \frac{1}{2\hat{\rho}} \{\hat{\rho}\alpha + (1-\alpha)\} \alpha (1-\alpha) \frac{\partial}{\partial \hat{t}} (\hat{\mathbf{u}}_2 - \hat{\mathbf{u}}_1), \quad (6.16)$$

$$\frac{\partial \hat{\mathbf{u}}_2}{\partial \hat{t}} = -\hat{\rho} \hat{\nabla} \hat{p} - \frac{1}{2} \{\hat{\rho}\alpha + (1-\alpha)\} \alpha \frac{\partial}{\partial \hat{t}} (\hat{\mathbf{u}}_2 - \hat{\mathbf{u}}_1). \quad (6.17)$$

Equations (6.16) and (6.17) are linear in the three unknowns $\hat{\nabla} \hat{p}$, $\partial \hat{\mathbf{u}}_1 / \partial \hat{t}$ and $\partial \hat{\mathbf{u}}_2 / \partial \hat{t}$, and we can easily show that

$$\frac{\partial}{\partial \hat{t}} \{\alpha \hat{\mathbf{u}}_1 + (1-\alpha) \hat{\mathbf{u}}_2\} = -\frac{\hat{\nabla} \hat{p}}{k(\alpha)}, \quad (6.18)$$

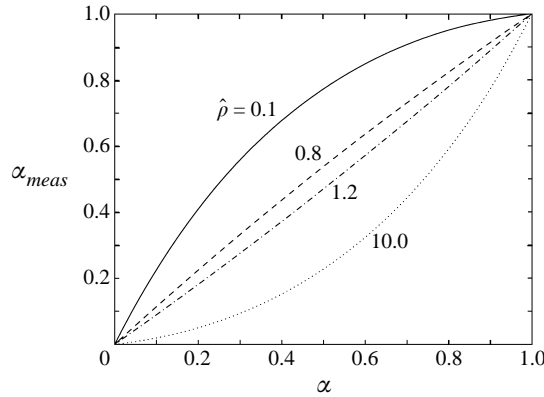


FIGURE 7. The measured fraction of the continuous fluid as a function of the actual fraction for $\hat{\rho} = 0.1, 0.8, 1.2, 10$ when α is constant.

where

$$k(\alpha) = \frac{3 - 2(1 - \hat{\rho})\alpha + (1 - \hat{\rho})^2\alpha^2}{3\hat{\rho} + (2 - \hat{\rho})(1 - \hat{\rho})\alpha}. \tag{6.19}$$

Equations (6.9) and (6.18) show that \hat{p} satisfies

$$\hat{\nabla} \cdot \left\{ \frac{\hat{\nabla} \hat{p}}{k(\alpha)} \right\} = 0. \tag{6.20}$$

The boundary conditions on the normal component of the mixture velocity, $\alpha \hat{\mathbf{u}}_1 + (1 - \alpha) \hat{\mathbf{u}}_2$, at each of the solid surfaces gives

$$\frac{\partial \hat{p}}{\partial \hat{r}} = 0 \quad \text{at } \hat{r} = \hat{R}_C, \tag{6.21}$$

$$\frac{\partial \hat{p}}{\partial \hat{r}} = k(\alpha) e^{i\hat{\theta}} \cos \theta \quad \text{at } \hat{r} = 1. \tag{6.22}$$

The remaining boundary conditions at the solid surfaces are satisfied across a boundary layer.

If α is constant \hat{p} is harmonic, and the solution of (6.20) subject to boundary conditions (6.21) and (6.22) is

$$\hat{p} = \frac{k(\alpha) e^{i\hat{\theta}}}{1 - \hat{R}_C^2} \left(\hat{r} + \frac{\hat{R}_C^2}{\hat{r}} \right) \cos \theta. \tag{6.23}$$

Since the solution is simply a multiple of the single-phase solution (3.1), the effect of the pipe wall on the measured density is the same. The measured liquid fraction is independent of \hat{R}_C and given by

$$\alpha_{meas} = \frac{\alpha \{3 - (1 - \hat{\rho}) \alpha\}}{2\hat{\rho} + 1 + (1 - \hat{\rho}) \alpha}. \tag{6.24}$$

Figure 7 shows $\alpha_{meas}(\alpha)$ for various values of the density ratio, $\hat{\rho}$. As we have found in the other idealized situations that we have studied, the error is much greater when the density ratio is large or small, and $\alpha_{meas}/\alpha \rightarrow 1$ as $\hat{\rho} \rightarrow 1$. When the density ratio is large or small the inertial forces generated by the relative motion of the two phases

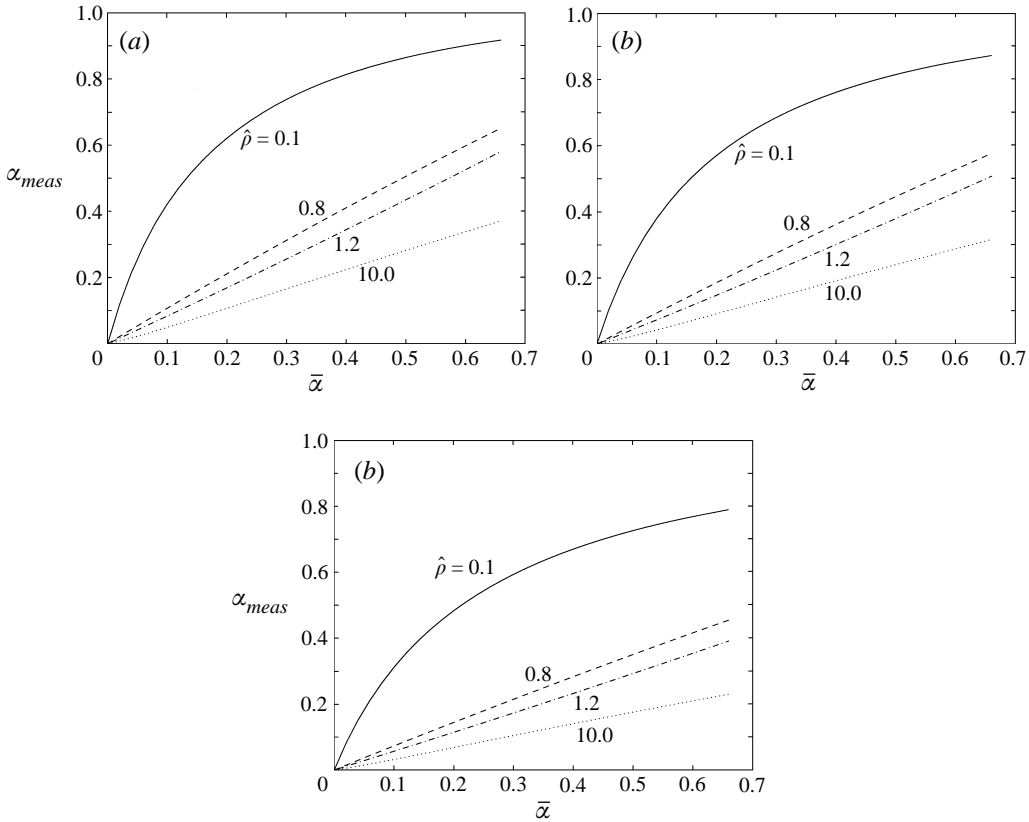


FIGURE 8. The measured fraction of the continuous fluid as a function of the actual fraction for $\hat{\rho} = 0.1, 0.8, 1.2, 10$ when α varies quadratically with \hat{r} and (a) $\hat{R}_C = 2$, (b) $\hat{R}_C = 3$, (c) $\hat{R}_C = 5$.

are sufficiently large to invalidate the simple interpretation. This is not simply due to the interphase added mass force. Indeed the difference between α_{meas} and α is even greater if the added mass force is neglected, since it acts to decrease the amplitude of the relative motion between the two fluids.

As an example of a spatially non-uniform distribution of fluids we consider the distribution

$$\alpha(\hat{r}) = \frac{6\bar{\alpha}(\hat{R}_C - \hat{r})(\hat{r} - 1)}{(\hat{R}_C - 1)^2}. \tag{6.25}$$

The fraction of fluid 1 varies quadratically with \hat{r} and $\alpha = 0$ at the rod and the pipe wall. The mean value of α is $\bar{\alpha}$. Note that we must restrict our attention to $0 \leq \bar{\alpha} \leq 2/3$ in order to ensure that $\alpha \leq 1$ everywhere. We seek a solution of the form

$$\hat{p} = e^{it} \cos \theta f(\hat{r}). \tag{6.26}$$

On substituting this into equation (6.20) and boundary conditions (6.21) and (6.22) we obtain

$$f'' + \left(\frac{1}{\hat{r}} - \frac{1}{k(\alpha)} \frac{dk}{d\alpha} \frac{d\alpha}{d\hat{r}} \right) f' - \frac{1}{\hat{r}^2} f = 0, \tag{6.27}$$

subject to

$$f' = 0 \quad \text{at } \hat{r} = \hat{R}_C, \quad (6.28)$$

$$f' = 1/\hat{\rho} \quad \text{at } \hat{r} = 1. \quad (6.29)$$

We can easily solve this two-point boundary value problem using the NAG routine D02GBF, and hence determine the fraction of liquid 1 measured by the device as

$$\alpha_{meas} = \left\{ 1 + \hat{\rho} \left(\frac{\hat{R}_C^2 - 1}{\hat{R}_C^2 + 1} \right) f(1) \right\} / (1 - \hat{\rho}). \quad (6.30)$$

Figure 8 shows how the measured fraction of liquid 1 varies as a function of the actual mean fraction, $\bar{\alpha}$, for various values of $\hat{\rho}$ and \hat{R}_C . When $\hat{R}_C = 2$ (figure 8a) and $\hat{\rho} = 0.8$ or 1.2 the measured fraction is close to the actual fraction, whilst for $\hat{\rho} = 0.1$ or 10 there is a significant error. When $\hat{R}_C = 3$ or 5 (figures 8b and 8c) the measured value is significantly lower in each case than when $\hat{R}_C = 2$, since the device is most sensitive to the fluid close to the surface of the rod, where the liquid fraction is lower than the mean value.

7. Conclusion

In this paper we have studied the response of an idealized system that has many of the features of a vibrating-element density meter operating in a two-phase flow. We have interpreted the results by assuming that the meter is operating in a single-phase fluid with density equal to that of the multiphase mixture. The main conclusion we can reach is that, if there is a significant density difference between the two phases, this interpretation produces unacceptably large errors. In practice, for particular cases where the likely disposition of the two phases is known in advance, for example slug flow or bubbly flow, a multiphase interpretation of such a meter may be possible, since in realistic cases the amplitude of the force on the device is likely to vary monotonically with mixture density. However, we have clearly shown that the resonance peak will not lie at the same frequency as it would for a single fluid with the same mean density. When the densities of the two fluids are comparable, for example in a flow of oil and water, the single-phase interpretation gives good results. However, we must note that this suffers from the same problem as any device that measures mixture density, for example a simple gradiomanometer. The calculation of α_{meas} involves the ratio of two small quantities and can easily be degraded by small measurement errors.

If the vibrating element has a typical lengthscale R , we have seen that it responds mainly to the fluids within a few multiples of R away. In addition, the response is spatially non-uniform with distance from the device, with the fluids at its surface having the greatest effect on the response. The most extreme case is when a thin layer of gas on the surface of the vibrating element masks the presence of any denser fluid further away. This suggests that some sort of flow conditioning is probably necessary in order to make the mixture as spatially homogeneous as possible if the simple interpretation is to be used.

I would like to thank Professor J. R. A. Pearson for suggesting this problem to me, and Professor A. C. King for his help in tidying up my finite Mellin transforms. Most of this work was done whilst I was an employee of Schlumberger Cambridge Research.

REFERENCES

- BETT, K. E., PALAVRA, A. M. F., RETSINA, T., RICHARDSON, S. M. & WAKEHAM, W.A. 1989 A vibrating-rod densimeter. *Intl J. Thermophys.* **10**, 871–883.
- CUMBERBATCH, E. & WILKS, G. 1987 An analysis of a vibrating element densitometer. *Math. Engng Ind.* **1**, 47–66.
- DREW, D. A. 1983 Mathematical modelling of two phase flow. *Ann. Rev. Fluid Mech.* **15**, 261–291.
- ISHII, R., UMEDA, Y., MURATA, S. & SHISHIDO, N. 1993 Bubbly flows through a converging-diverging nozzle. *Phys. Fluids A* **5**, 1630–1643.
- PAUCHON, C. & BANERJEE, S. 1986 Interphase momentum interaction effects in the averaged multifield model. *Intl J. Multiphase Flow* **12**, 559–573.
- RETSINA, T., RICHARDSON, S. M. & WAKEHAM, W. A. 1986 The theory of a vibrating-rod densimeter. *Appl. Sci. Res.* **43**, 127–158.
- SNEDDON, I. N. 1972 *The Use of Integral Transforms*, pp. 462–467. McGraw–Hill.
- WATT, R. M. & LU, W. 1992 CFD analysis of fluid effects in coriolis mass flowmeters. *Proc. North Sea Flow Measurement Workshop*.